ELECTRON BEAM REMELTING OF PLASMA SPRAYED ALUMINA COATINGS

MATĚJÍČEK Jiří[1], VEVERKA Jakub[1,2], ČÍŽEK Jan[3], KOUŘIL Jan[3]

[1]*Institute of Plasma Physics, Prague, Czech Republic, EU*
[2]*Faculty of Nuclear Sciences and Physical Engineering, Czech Technical University in Prague, Czech Republic, EU*
[3]*NETME Centre, Institute of Materials Science and Engineering, Brno University of Technology, Brno, Czech Republic, EU*

Abstract

Plasma sprayed alumina coatings find numerous applications in various fields, where they enhance the properties of the base material. Examples include thermal barriers, wear resistance, electrical insulation, and diffusion and corrosion barriers. A typical structure of plasma sprayed coatings, containing a multitude of voids and imperfectly bonded interfaces, gives them unique properties - particularly low thermal conductivity, high strain tolerance, etc. However, for certain applications such as permeation barriers or wear resistance, these voids may be detrimental.

This paper reports on the first experiments with remelting of plasma sprayed alumina coatings by electron beam technology, with the purpose of densifying the coatings and thereby eliminating the voids. Throughout the study, several parameters of the e-beam device were varied - beam current, traverse velocity and number of passes. The treated coatings were observed by light and electron microscopy and the thickness, structure and surface morphology of the remelted layer were determined and correlated with the process parameters. Based on the first series of experiments, the e-beam settings leading to dense and smooth remelted layer of sufficient thickness were obtained. In this layer, a change of phase composition and a marked increase in hardness were observed.

Keywords: Plasma sprayed coating, alumina, electron beam, remelting, post-treatment

1. INTRODUCTION

Plasma sprayed coatings are being used in numerous applications in various fields, where they enhance the properties of the base material. The process consists of introducing the powder into a plasma jet, which melts and accelerates the particles towards a substrate where they flatten and solidify, thereby forming the coating. This results in a typical lamellar structure - besides the flattened particles, called ‘splats’, it contains a multitude of voids and interfaces [1]. As a consequence, the coatings feature unique properties - particularly low thermal conductivity, low stiffness, high strain tolerance, etc. [2, 3]. Among the ceramic coatings, alumina is a particularly versatile material whose applications include thermal barriers, wear resistance, electrical insulation, and diffusion and corrosion barriers. While for thermal barriers, the presence of pores and interfaces is beneficial (by reducing the thermal conductivity), for other applications such as permeation barriers [4] or wear resistance, the voids may be detrimental.

Several studies have been conducted, focusing on post-treatment of plasma sprayed coatings with the aim of reducing or eliminating the porosity and improving particular properties. Laser treatment of plasma sprayed grey alumina and zirconia was explored in [5]. In zirconia coatings, marked increase in hardness and wear resistance was observed, although some horizontal cracks were formed; in alumina, only minor modification of the structure and properties was observed. Laser treatment of alumina-chromia coatings [6] resulted in densification, increased hardness and homogenization even of coatings produced from mechanical mixtures. Laser-treated white and grey alumina coatings [7] also featured increased hardness and wear resistance. Moreover, the initial coating composition influenced the remelted depth as well as the observed phase

transformations. Laser remelted plasma sprayed tungsten coatings featured smooth and dense remelted layers with eliminated voids and cracks, and a marked increase in thermal conductivity, despite limited remelted depth [8]. Electron beam remelting of HVOF- and cold-sprayed CoNiCrAlY coatings resulted in densification, reduction in hardness, increase in Young's modulus and strong interdiffusion across the substrate/coating interface, replacing a sharp step with a smooth transient [9].

This study is focused on remelting of plasma sprayed alumina by an electron beam. The paper reports on the first stage of process optimization and basic characterization of the treated coatings.

2. EXPERIMENTAL DETAILS

Alumina coatings were prepared by plasma spraying using a WSP-H torch with argon-water stabilization (Institute of Plasma Physics, Prague). Surprex AW24 powder (Fujimi, Japan) with a 63-100 μm size range was used as a feedstock. Feeding distance was 65 mm, spraying distance was 360 mm, feed rate was 10 kg/h. 2.5 mm thick low carbon steel preheated to 100 °C was used for substrates. Three series of samples were prepared, varying in thickness of the alumina layer (approximately 100 μm, 200 μm and 300 μm). The electron beam post-treatment was performed using K26 system (Pro-beam, Germany) consisting of an electron gun, vacuum chamber and multi-axis positioning system. The experimental matrix involved the variation of the following parameters: beam current, traverse velocity and number of passes. Voltage of 120 kV and beam diameter of 20 mm were used in all cases. The individual parameter combinations are listed in **Table 1.**

Table 1 Parameters of the remelting experiments; t = as-sprayed coating thickness, I = remelting current, v = beam traverse velocity, n = number of beam passes. In the sample labels, the first digit denotes the e-beam parameters (I, v), the second digit the coating thickness and the letter one or two passes.

Sample	t [μm]	I [mA]	v [mm/s]	n	Sample	t [μm]	I [mA]	v [mm/s]	n
1-1-A	100	10	5	1	8-1-A	100	6	40	1
2-1-A	100	8	5	1	8-1-B	100	6	40	2
3-1-A	100	12	5	1	8-2-A	200	6	40	1
4-1-A	100	6	5	1	8-2-B	200	6	40	2
4-1-B	100	6	5	2	8-3-A	300	6	40	1
5-1-A	100	8	7	1	8-3-B	300	6	40	2
5-1-B	100	8	9	1	9-1-A	100	3	20	1
6-1-A	100	6	20	1	9-1-B	100	3	20	2
6-1-B	100	6	20	2	9-2-A	200	3	20	1
7-1-A	100	6	2	1	9-2-B	200	3	20	2
7-1-B	100	6	2	2	9-3-A	300	3	20	1
6-2-A	200	6	20	1	9-3-B	300	3	20	2
6-2-B	200	6	20	2	10-2-A	200	9	20	1
6-3-A	300	6	20	1	10-2-B	200	9	20	2
6-3-B	300	6	20	2	10-3-A	300	9	20	1
					10-3-B	300	9	20	2

The general aim was to eliminate the original pores and to obtain a smooth and contiguous remelted layer. To achieve the goal, the optimization was performed in two stages. In the first stage, using only 100 μm thick coatings, the parameters were varied in a relatively broad range, to get acquainted with the response of the material to their variation. The surface and polished cross sections of the treated samples were observed in a light microscope. Based on these observations, the most promising settings were used in the second stage:

varied in a narrower range and applied to coatings of all three thicknesses. The surface and polished cross sections of selected samples were observed in an EVO MA15 scanning electron microscope (Carl Zeiss SMT, Germany). The observations focused on the morphology (roughness/smoothness, contiguity) and thickness of the remelted layer and the presence/absence of pores and cracks. X-ray diffraction was performed on selected untreated and treated samples, using a Discover D8 diffractometer (Bruker, Germany) with Cu radiation. For phase analysis, Rietveld refinement of the full pattern was carried out. Vickers microhardness of treated and untreated regions of several samples was determined on a Nexus 4504 hardness tester (Innovatest, Netherlands) with a Vickers indentor, 100 g load and 10 s dwell time.

3. RESULTS

While a large number of observations was made, only selected results will be presented here, illustrating the significant trends. A comprehensive set of results was compiled in [10]. The treated samples exhibited a different degree of melting, contiguity, morphology and thickness of the remelted layer. An example of the non-optimized settings, illustrating the effect of initial coating thickness and number of passes, is shown in **Figure 1**. Sample 9-1-A exhibits almost unaffected surface, indicating that the electron beam power was insufficient. In the cross-section, few isolated remelted islands were observed. For a double-pass treatment (sample 9-1-B), the ratio of the remelted area increased and the remelted depth reached about 30 μm. For thicker coatings (samples 9-2-B and 9-3-B), the degree of melting increased further, although the maximum remelted depth increased only locally. This indicates an effect of the coating thickness - while for thin coatings, a significant portion of the incident heat from the laser is transferred to the steel substrate, for thicker coatings, the deeper layers act as thermal barrier, concentrating the heat at the surface and promoting the surface melting.

Figure 2. shows the surface morphology and cross sections of samples 6-3-A and 6-3-B, where the parameters resulting from the first stage of optimization were applied on the 300 μm coating. Sample 6-3-A features a smooth remelted layer covering almost 100% of the surface, with few localized imperfections/depressions only. Remelting of 6-3-B was successful on the whole surface, but noticeable vertical cracks occurred. On the cross sections, a clear distinction of the unaffected and remelted regions can be made. The as-sprayed coatings contain numerous voids - nearly equiaxed pores, horizontal voids (unbonded interfaces between splats), and vertical microcracks. In the remelted layer, these features are eliminated, resulting in a dense layer with only few isolated vertical cracks. These appear as a consequence of the thermal gradient and post-treatment shrinkage of the top surface. Typical thickness of the remelted layer was 60 to 80 μm.

Samples 10-3-A and 10-3-B, resulting from the second stage of optimization, featured the largest remelted depth of all examined specimens. As can be seen in **Figure 3**, the surface of 10-3-A was continuous: very few depressions occurred, but none of them reached the steel substrate. Cross section shows a smooth, slightly wavy surface; typical remelted depth varied between 70 and 100 μm, reaching up to 150 μm in some areas. The surface of 10-3-B was smooth and contiguous, too; few cracks occurred, but very distant in comparison with earlier specimens. The surface profile was quite straight; the remelted depth layer was also more even, between 120 to 150 μm.

Analysis of the x-ray diffraction spectra indicated that the as-sprayed coatings contained about 29 wt% of amorphous phase; the crystalline phase consisted of 86 wt% of gamma-alumina and 14 wt% of alpha-alumina. Gamma-alumina is a metastable phase whose presence is typical for plasma sprayed alumina; its formation results from the rapid solidification following the impact of the molten droplets on a much colder substrate. The remelted layer in samples 10-3-B and 6-3-B consists of stable alpha-alumina only, indicating significantly slower solidification after the remelting. Hardness of the as-sprayed and remelted regions of selected samples is shown in **Table 2**. Hardness of the remelted layers is 2-3 times greater than that of the as-sprayed counterparts, indicating a remarkable effect of the pore and crack elimination.

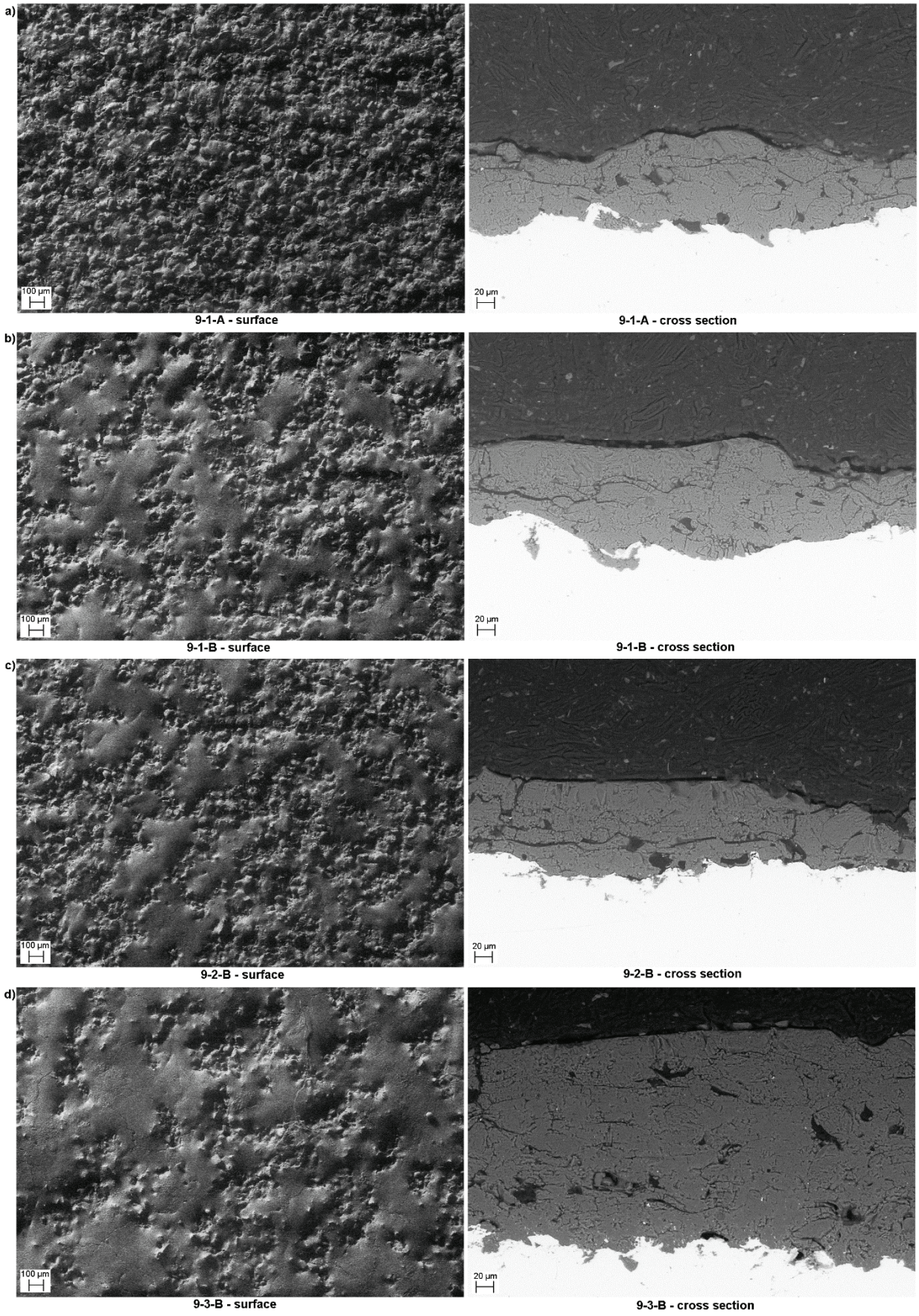

Figure 1 Surface morphology and cross sections of samples a) 9-1-A, b) 9-1-B, c) 9-2-B, d) 9-3-B

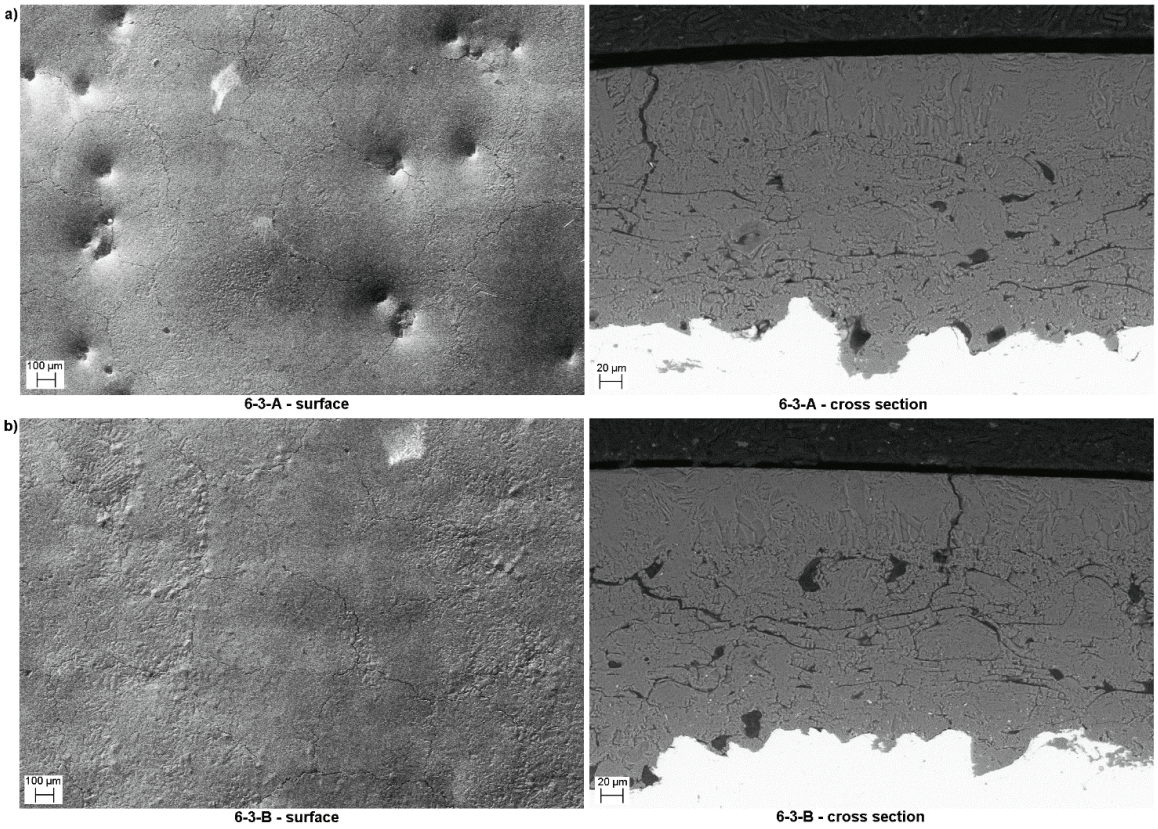

Figure 2 Surface morphology and cross sections of samples a) 6-3-A, b) 6-3-B

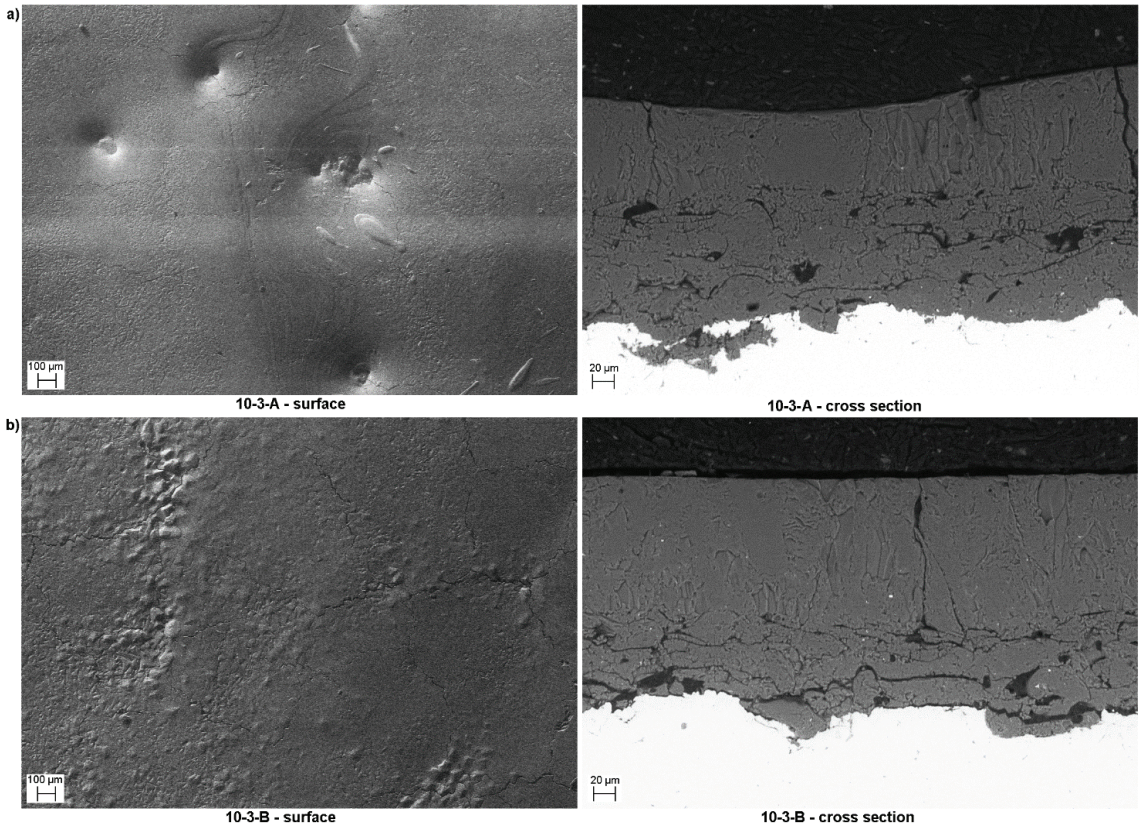

Figure 3 Surface morphology and cross sections of samples a) 10-3-A, b) 10-3-B

Table 2 Vickers hardness (HV - 100 g load, 10 s dwell) of as-sprayed and remelted regions of selected samples

sample	as-sprayed	remelted
6-3-B	804 ± 69	2491 ± 52
8-3-B	761 ± 62	2468 ± 146
9-3-B	1190 ± 41	2459 ± 88
10-3-B	719 ± 71	1910 ± 78

4. CONCLUSIONS

The experiments confirmed that electron beam is capable of remelting and densifying plasma sprayed alumina coatings by eliminating the pores and cracks characteristic for the as-sprayed structure. The effects of various process parameters (beam current, traverse velocity, number of passes) and the initial coating thickness on the extent of melting and morphology of the treated surface were studied. Based on these observations, initial optimization of the process was performed, resulting in dense, smooth and contiguous remelted layers. Few vertical cracks were still present, though, as a result of post-treatment shrinkage of the remelted layer. Generally, the ratio of remelted to unaffected thickness increased with increasing number of passes, increasing current and decreasing velocity, although at higher currents and lower velocities, the number of cracks increased. The maximum remelted depth reached up to 150 μm. Remelting of the entire sprayed coating was not achieved in this stage. Further optimization of the process is underway. A remarkable increase in hardness in the remelted layer was demonstrated. This could be attributed primarily to the elimination of the voids, possibly also to the change in phase composition.

ACKNOWLEDGEMENTS

This work was supported by Czech Science Foundation through grant no. 14-12837S and FME BUT specific research project FSI-S-14-2427. The work was further supported by Czech Ministry of Education, Youth and Sports through the project NETME Centre PLUS (LO1202) under the National Programme for Sustainability.

REFERENCES

[1] PAWLOWSKI, L. *The science and engineering of thermal spray coating.* John Wiley & Sons, 1995. 432p.

[2] VILÉMOVÁ, M., MATĚJÍČEK, J., MUŠÁLEK, R., NOHAVA, J. Application of Structure-Based Models of Mechanical and Thermal Properties on Plasma Sprayed Coatings. *Journal of Thermal Spray Technology,* 2012, vol. 21, no. 3-4, pp. 372-382.

[3] MUŠÁLEK, R., MATĚJÍČEK, J., VILÉMOVÁ, M., KOVÁŘÍK, O. Non-Linear Mechanical Behavior of Plasma Sprayed Alumina Under Mechanical and Thermal Loading. *Journal of Thermal Spray Technology,* 2010, vol. 19, no. 1-2, pp. 422-428.

[4] SAMPLE, T., PERUJO, A., KOLBE, H., MANCINELLI, B. The Hydrogen Permeation Behaviour of Aluminised Coated Martensitic Steels Under Gaseous Hydrogen, Liquid Pb-17li/Hydrogen and Cyclic Tensile Load. *Journal of Nuclear Materials,* 2000, vol. 283, pp. 1272-1276.

[5] CTIBOR, P., KRAUS, L., TUOMINEN, J., VUORISTO, P., CHRÁSKA, P. Improvement of Mechanical Properties of Alumina and Zirconia Plasma Sprayed Coatings Induced by Laser Post-Treatment. *Ceramics-Silikáty,* 2007, vol. 51, no. 4, pp. 181-189.

[6] DUBSKÝ, J., KOLMAN, B., CHRÁSKA, P., JANČÁREK, A. Laser post-treatment of plasma sprayed Al_2O_3-Cr_2O_3 coatings. In *Thermal Spray 2006: Science, Innovation, and Application*. ASM International, 2006, paper no. s15_7-11989.

[7] YANG, Y. Z., ZHU, Y. L., LIU, Z. Y., CHUANG, Y. Z. Laser Remelting of Plasma Sprayed Al_2O_3 Ceramic Coatings and Subsequent Wear Resistance. *Materials Science and Engineering A,* 2000, vol. 291, no. 1-2, pp. 168-172.

[8] MATĚJÍČEK, J., HOLUB, P. Laser Remelting of Plasma-Sprayed Tungsten Coatings. *Journal of Thermal Spray Technology,* 2014, vol. 23, no. 4, pp. 750-754.

[9] ČÍŽEK, J., MATĚJKOVÁ, M., KOUŘIL, J., ČUPERA, J., DLOUHÝ I. Potential of New-Generation Electron Beam Technology in Interface Modification of Cold and HVOF Sprayed MCrAlY Bond Coats. *Advances in Materials Science and Engineering,* 2016, paper no. 9070468.

[10] VEVERKA, J. *Materials for permeation barriers.* Research report, Czech Technical University in Prague, 2016. 40p.